Thermographic real-time-monitoring of surgical radiofrequency and microwave ablation in a perfused porcine liver model

FLORIAN PRIMAVESI[1,2], STEFAN SWIERCZYNSKI[2], ECKHARD KLIESER[3], TOBIAS KIESSLICH[4], TARKAN JÄGER[2], ROMANA URBAS[3], JÖRG HUTTER[2], DANIEL NEUREITER[3], DIETMAR ÖFNER[1] and STEFAN STÄTTNER[1]

[1]Department of Visceral, Transplant and Thoracic Surgery, Center of Operative Medicine, Medical University Innsbruck, A-6020 Innsbruck; [2]Department of Surgery; [3]Institute of Pathology; [4]Department of Internal Medicine I, Paracelsus Medical University, A-5020 Salzburg, Austria

Received September 18, 2017; Accepted November 21, 2017

DOI: 10.3892/ol.2017.7634

Abstract. Radiofrequency ablation (RFA) and microwave ablation (MWA) are currently the dominant modalities to treat unresectable liver tumors. Monitoring the ablation process with b-mode-sonography is often hampered by artefacts. Furthermore, vessels may cause cooling in the adjacent tumor target (heat-sink-effect) with risk of local recurrence. The present study evaluated infrared-thermography to monitor surgical RFA/MWA and detect heat-sink-effects in real-time. RFA and MWA of perfused porcine livers was conducted at peripheral and central-vessel-adjacent locations, and monitored by real-time thermography. Ablation was measured and evaluated by gross pathology. The mean time for ablation was significantly longer in RFA compared with MWA (8 vs. 2 min). Although mean macroscopic ablation diameter was similar (RFA, 3.17 cm; MWA, 3.38 cm), RFA showed a significant heat-sink-effect compared with MWA. The surface temperature during central RFA near vessels was 1/3 lower compared with peripheral RFA (47.11±8.35˚C vs. 68.72±12.70˚C; P<0.001). There was no significant difference in MWA (50.52±8.35˚C vs. 50.18±10.35˚C; P=0.74). In conclusion, thermography is suitable to monitor the correct ablation with MWA and RFA. The results of the current study demonstrated a significant heat-sink-effect for RFA, but not MWA near vessels. MWA reaches consistent surface temperatures much faster than RFA. With further *in vivo* validation, thermography may be useful to ensure appropriate ablation particularly near vulnerable or vascular structures.

Correspondence to: Dr Florian Primavesi, Department of Visceral, Transplant and Thoracic Surgery, Center of Operative Medicine, Medical University Innsbruck, Anichstrasse 35, A-6020 Innsbruck, Austria
E-mail: florian.primavesi@tirol-kliniken.at

Abbreviations: CEUS, contrast-enhanced ultrasound; CT, computed tomography; FFPE, formalin-fixed paraffin-embedded tissue; FLR, future liver remnant; MRI, magnetic resonance imaging; MWA, microwave ablation; MW, microwave; NormV, surrounding parenchyma surface temperature (near vessel); NormP, surrounding parenchyma surface temperature (peripheral); PBS, sodium phosphate buffer solution; RFA, radiofrequency ablation

Key words: radiofrequency ablation, microwave ablation, liver, surgery, thermography, porcine model, monitoring

Introduction

Surgical resection remains the gold standard therapy for primary and secondary liver malignancies, but resectability largely depends on factors such as extent of the disease, concurrent liver steatosis or cirrhosis, amount of remaining healthy liver tissue after resection (the future liver remnant-FLR) as well as patient comorbidities. Therefore, thermal ablation is widely used as an alternative or additional technique in cases were resection deems hazardous, or in unresectable disease with multiple lesions when only the combined ablation-and-resection (1) or two-stage hepatectomy approach seems feasible to achieve tumor-free margins with sufficient FLR.

The two currently most common thermal ablation modalities are radiofrequency ablation (RFA) and microwave ablation (MWA) (2,3), both applied either percutaneously or during open or laparoscopic surgery (‘surgical ablation’) (4). In RFA an electrical current within the radiofrequency range is transported through either a monopolar electrode or between two bipolar electrodes to produce heat-induced cytotoxicity in the liver tissue (5,6). MWA technique is different, as microwave radiation leads to high frequency oscillation in water molecules, subsequent frictional heating and cell death through coagulation necrosis (4,7). Therefore, MWA requires no application of grounding pads because an electrical circuit is not established. MWA is mostly applied through a single coaxial electrode device (3,4,8,9).

The success of thermal ablation (complete necrosis of tumors) generally depends on multiple factors like tumor size, location, hepatic blood flow and equipment selection (3,7,10). In this regard, previous research revealed several advantages of MWA compared to conventional (monopolar) RFA, namely easier and fast use with superior heating capacity,

independency of tissue charring and only minimal influence of the 'heat-sink-effect'. This term describes cooling within ablation zones next to large hepatic blood vessels which might lead to incomplete tumor necrosis resulting in local recurrence (8).

In general, correct image-guided insertion of electrodes is crucial to achieve a successful ablation with completely devitalized tumors. While in percutaneous radiological ablation this is either achieved by computed tomography or sonography, surgical ablation relies heavily on intraoperative B-mode ultrasound. Although this can be a very powerful tool in experienced hands, differentiation of viable and destructed tissue and identification of the tumor border is quite challenging in daily practice-mainly due to tissue scarring and gas bubble phenomena which arise during the ablation process. Therefore several other imaging techniques such as contrast-enhanced sonography (11), real-time ultrasound elastography (12) and electrode vibration elastography (13) were already evaluated to further enhance the security and practicability of ablations. This experimental study for the first time examines the feasibility of infrared thermographic monitoring in RFA and MWA.

Thermographic imaging uses radiation within the long-infrared range of the electromagnetic spectrum (9-14 μm) that is emitted by all objects. Hereby, colored output images with analyzable information of surface temperatures are obtained. It is non-invasive, easy to apply and technically well-engineered due to its wide range use in medicine (e.g., to detect inflammation by irregular cutaneous blood flow) and several other industries such as construction technology (e.g., to analyze heat leaks in thermal insulation) (14).

In this proof-of-principle study we hypothesize, that thermography: i) is a suitable non-invasive tool for monitoring the ablation process; and ii) is also helpful to detect a possible heat-sink effect near large vessels. Hence, we compared RFA to MWA using an *ex vivo* perfused porcine liver model.

Materials and methods

We investigated each ablation technology in a setting with both a heat sink and non-heat sink surrounding. Therefore, an experimental setting using *ex vivo* perfused porcine livers with hepatic flow simulation was established (Fig. 1A and B). Since no patients or living animals were involved no ethics approval was required according to local regulations.

Experimental and technical setup. Four complete, freshly taken porcine livers from adult animals with intact in- and outflow vessels were obtained from an abattoir and instantly used after less than 1-h cooled transport. Perfusion at body temperature was initiated by placing the livers in a metal container half filled with 37˚C PBS (standardized sodium phosphate buffer), keeping the temperature constant with a heating system. A temperature probe continuously controlled temperature levels and the heating system was adjusted accordingly. Hepatic inflow was simulated through flexible rubber-tubes sutured to the portal vein and connected to a perfusion pump system (Heissner P300-I; Heissner GMBH, Lauterbach, Germany). Hereby a constant hepatic flow with 5.3 liters per min was established to emulate the average human cardiac output. A thermographic camera (FLIR A35sc; FLIR, Wilsonville, Oregon, USA) was centered 50 cm above the liver in a right angle. Calibrations for emissivity, distance, relative humidity and ambient temperature were set according to the manufacturers recommendations.

For RFA a 250-watt radiofrequency generator (Model 1500X) was equipped with an expandable, multi-array monopolar RFA electrode (StarBurst XL RFA Device; both RITA Medical Systems, Fremont, CA, USA;/AngioDynamics Inc., Latham, NY, USA). MWA was applied using a 2.45 GHz microwave generator (Sulis VpMTA Generator with Local Control Station) with a single-monopolar applicator-needle (Accu2i pMTA Applicator; both Microsulis Medical Ltd., Denmead, UK/AngioDynamics Inc.) (Fig. 1C).

Experimental workflow. We sequentially performed a central and peripheral ablation with MWA in one hepatic lobe and RFA in the other contralateral lobe in each of the four livers. To assess the influence of a possible heat sink effect, a central ablation with a distance of 1 cm from the tip of the needle to the wall of the main right or left portal vein branch was compared to a peripheral ablation with the probe tip located 3 cm from the hepatic margin (Fig. 1B). In both settings, the probe tip was placed in a parenchymal depth of 3 cm below the liver surface. Sonographic guidance was used for needle placement in both locations and exclusion of nearby large vessels in the peripheral setting.

Before starting and during the ablation process, the surface temperature of non-affected central liver parenchyma and the surrounding peripheral PBS buffer temperature were documented as baseline values (NormV/NormP). MWA device was set to 2 min ablation time with 100 Watt, RFA to 150 Watt for 8 min including a maximum of 3 min pre-heating to reach operating temperature (set to 105˚C). After the heat-up time of 3 min the RFA needle was extended to the full antenna length.

All ablative procedures were constantly monitored with the thermographic camera in real-time. After every ablative run, the parenchyma was dissected vertically along the ablation needle axis and the maximum diameter of the macroscopically clearly marked ablation zone was measured with a linear centimeter scale (Fig. 2). Tissue specimens of about 1 cm^3 size collected from the center and the macroscopic border were stored as formalin-fixed, paraffin-embedded (FFPE) specimens for routine histological staining with haematoxylin and eosin (H&E) to confirm the correct ablation process, the extent of ablation and morphological changes, especially grade of necrosis.

The documented thermographic images were evaluated concerning the temperature profiles using the manufacturer's professional infrared reporting software (FLIR Tools Plus software). Mean temperatures (with standard deviations) were calculated according to the scheme described in Fig. 3 with one central temperature point at the probe tip (X^1) and further four surrounding points at 50% of the maximum visible ablation diameter (X^{2-5}). Temperature points were measured every 10 sec (for 120 sec) for MWA and every 20 sec (for 480 sec) for RFA. Recorded radiometric data were exported and further statistically analyzed with SPSS Statistics 21 (IBM Corp., Armonk, NY, USA). Mean ablation infrared temperature levels were compared using the Student's t-test.

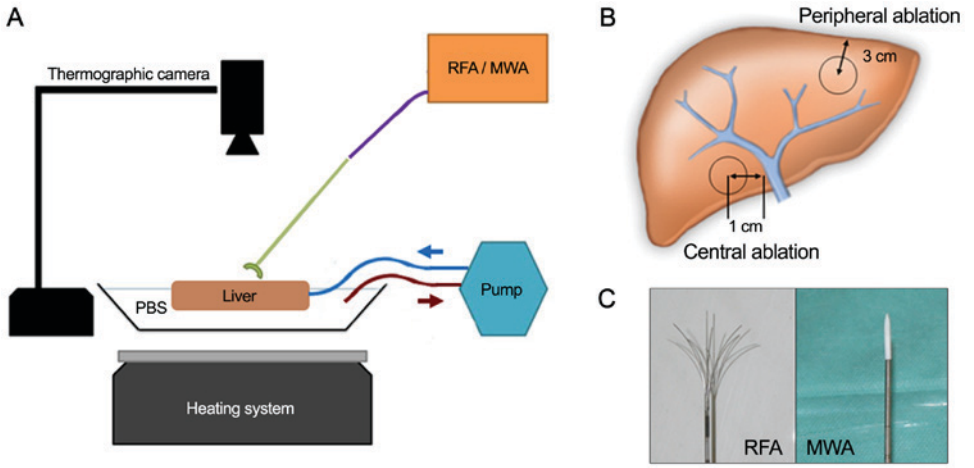

Figure 1. Experimental set up and equipment of the study. (A) Experimental set up. (B) For central ablations (MWA and RFA) the probe tip was placed 1 cm adjacent to the right or left main portal vein branch under ultrasound guidance. Peripheral ablations were performed with a distance of 3 cm from the probe tip to the hepatic edge. In both settings, the probe tip was placed in a parenchymal depth of 3 cm below the liver surface. (C) Multi-array monopolar RFA electrode (left) and monopolar MWA single-electrode (right). PBS, phosphate-buffered saline; RFA, radiofrequency ablation; MWA, microwave ablation.

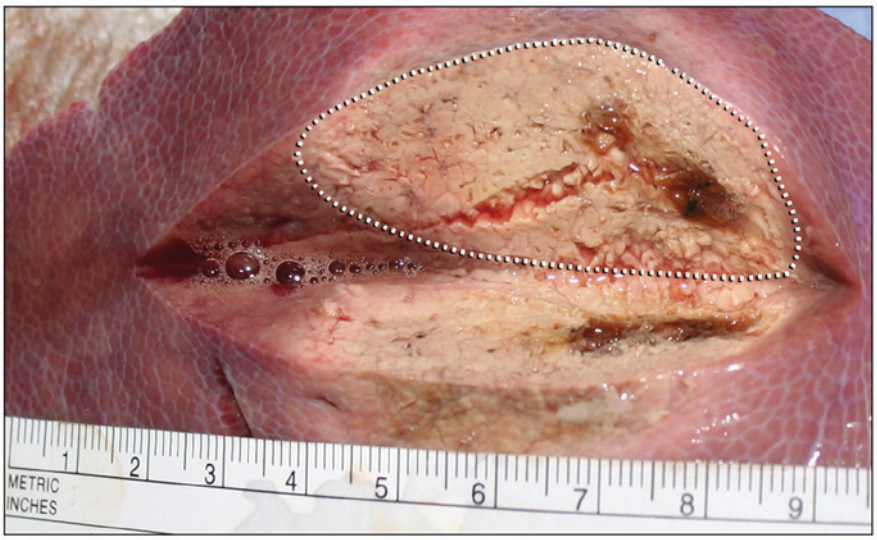

Figure 2. Example of hepatic microwave ablation. Photography of a peripheral liver tissue dissected after MWA. Note the rather elliptic shape of ablated areal (dotted line) compared to more spherical ablations with RFA (not shown). RFA, radiofrequency ablation; MWA, microwave ablation.

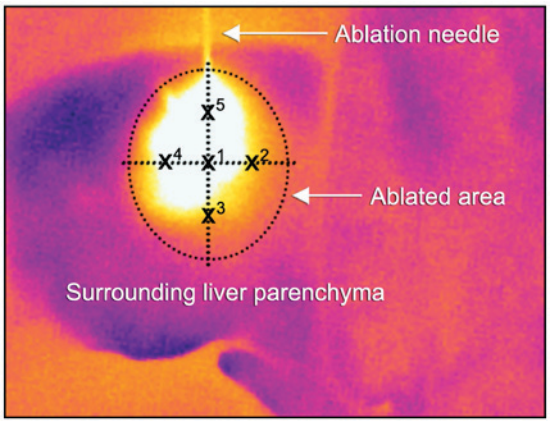

Figure 3. Thermographic temperature measurements model. Illustration of real-time infrared surface temperature measurements during an ongoing MWA. Values were calculated for each ablation by creating a mean value of temperatures at the ablation needle tip (X^1) and at 50% of the total ablation zone in each direction (X^{2-5}). MWA, microwave ablation.

Results

The experimental setup of MWA vs. RFA ablations in general showed comparable temperatures at the surrounding peripheral/central perivascular parenchyma of 33.43˚C (±-2.57)/32.53˚C (±-1.58) in MWA and 35.6˚C (±-3.16)/32.32˚C (±-1.23) in RFA, respectively. (Table I-MWA_NormP/NormV vs. RFA_NormP/NormV). The peripheral temperature in both techniques was higher due to increased heat transmission in the fluid surrounding. Representative examples of real-time thermography of an MWA and RFA ablative run are given in Figs. 4A, B and 5A.

MWA data. MW ablation showed homogenous temperature profiles and very short heat up time (Fig. 6 and Table I) in the peripheral (non-heat-sink) environment as well as in the central (heat-sink) location. When using the manufacturer's recommendation of 100 watts for 120 sec to achieve a

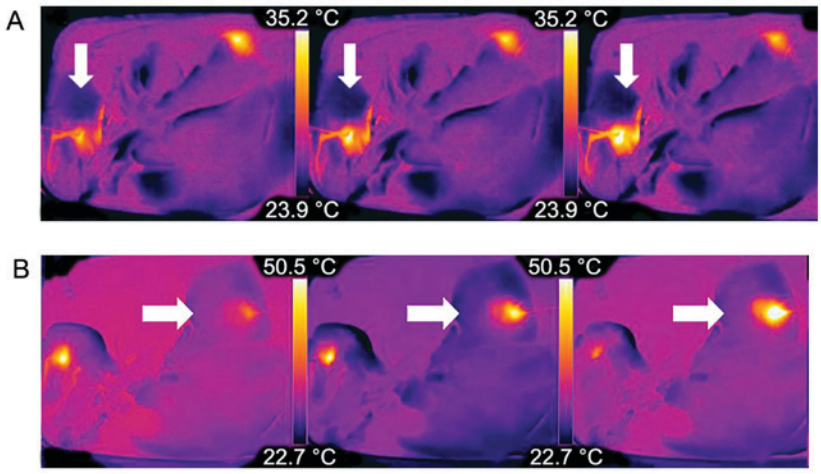

Figure 4. Examples of thermographic images. Real-time visualization of (A) MWA and (B) RFA each from left to right. (A) Example of the dynamics of central MWA near a large vessel; note the visible heat flow within the adjacent vessel (white arrow). (B) Dynamics of a peripheral RFA. RFA, radiofrequency ablation; MWA, microwave ablation.

predicted spherical ablation zone of 3 cm, the mean macroscopic ablation diameter was 3.38 cm (±0.26). Ablation in the liver periphery resulted in a diameter of 3.19 cm (±0.13) compared to 3.56 cm (±0.06) in proximity to a vessel. The mean surface temperature recorded was 50.18˚C (±10.35) in peripheral vs. 50.52˚C (±8.35) in central MW ablations (P=0.74). However, the temperature increased more stable and reached a higher end-point in the peripheral setting than in the central setting, which might indicate a minimal heat-sink effect in MWA. In general, the thermographic ablation zones were very clearly defined in the thermographic documentation and showed a homogenous round or slightly elliptic zone.

RFA data. RFA needs a considerable pre-heating time before antenna extensions to achieve appropriate target temperatures. When using the recommended settings of 150 Watt for 5 min (plus 3 min pre-heat time) for an anticipated lesion of 3 cm, the mean macroscopic ablation diameter was 3.17 cm (±0.09). Ablation in the liver periphery resulted in a diameter of 3.10 cm (±0.36) compared to 3.23 cm (±0.33) in proximity to a vessel. The mean surface temperature recorded was 68.72˚C (±12.70) in peripheral vs. 47.11˚C (±8.35) in central RFAs (P<0.001) (Fig. 6 and Table I). This indicates a stronger heat sink effect than in MWA. Furthermore, the temperature changes in peripheral and central RFA were much more pronounced compared to MWA, suggesting increased susceptibility of radiofrequency current to alterations in the surrounding area, such as charring or dessication (Fig. 7).

Histology. Histology confirmed correct ablation in both ablative techniques and microscopically verified the necrotic border of our macroscopic measurements. H&E-staining revealed increased cytoplasmic eosinophilia, cytoplasmic homogenization and destruction of vessel walls and ductular epithelium indicating liver tissue regression. These morphologic alterations could be recognized with a much greater extent within the samples taken from the ablation core. Although liver tissue in biopsies of healthy tissue outside the macroscopic border mainly preserved its histological tissue architecture some small portal tracts and vessel walls showed the same signs of regression as samples from the ablation core, suggesting a gradient partial cell damage beyond the visible border.

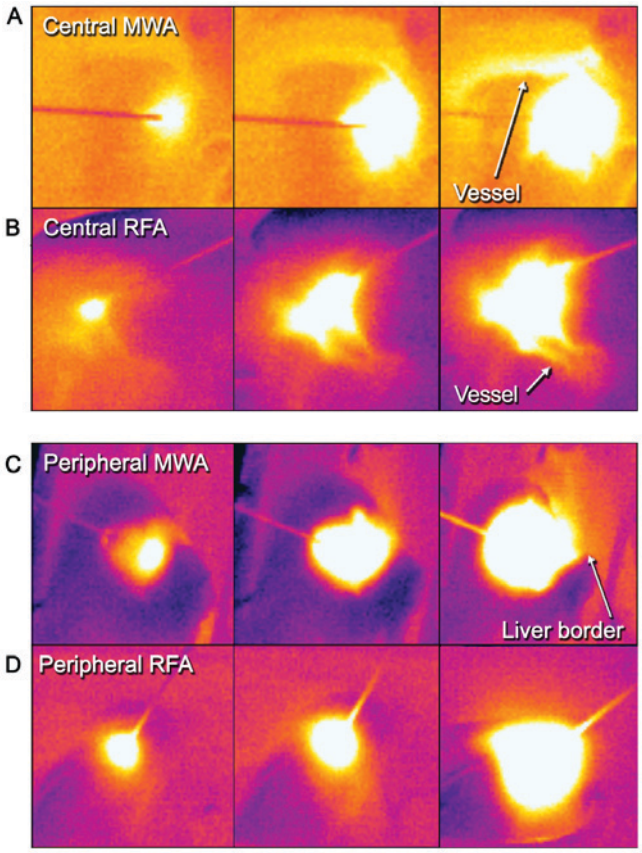

Figure 5. Thermography in central and peripheral ablations. From left to right: Comparative examples of a central (A) MWA and (B) RFA sequence to a peripheral (C) MWA and (D) RFA sequence. Note the adjacent vessels with a visible heat sink in both techniques but how the shape of central RFA changes compared to peripheral RFA. Further, note how heat transmission at the liver border is visualized and might help in preventing injuries at nearby structures/organs (peripheral MWA, right frame). RFA, radiofrequency ablation; MWA, microwave ablation.

Table I. Thermographic temperature measurements.

Measurement	N (measuring points[a])	Minimum (˚C)	Maximum (˚C)	Mean (˚C)	Standard deviation (˚C)
MWA_NormV	12	29.37	34.69	32.53	1.58
MWA_NormP	12	29.46	36.73	33.43	2.57
MWA_Ves	12	32.72	60.02	50.52	8.35
MWA_Peri	12	33.77	63.45	50.18	10.35
RFA_NormV	24	30.17	33.83	32.32	1.23
RFA_NormP	24	29.00	39.75	35.60	3.16
RFA_Ves	24	33.87	57.78	47.11	8.35
RFA_Peri	24	35.73	81.15	68.72	12.70

[a]The short running time of the MWA limited the measurements to n=12. *MWA_NormV*=central (near vessel) basic surrounding temperature near for MWA. *MWA_NormP*=peripheral basic surrounding temperature for MWA. *MWA_Ves*=temperature within the ablation area for central MWA. *MWA_Peri*=temperature within the ablation area for central RFA. Similar abbreviations apply for RFA. RFA, radiofrequency ablation; MWA, microwave ablation.

Discussion

To the best of our knowledge, the present study is the first to investigate the feasibility of thermography as a monitoring tool for open surgical hepatic MWA/RFA. Both ablation techniques induced visually well definable thermographic patterns. Within the ablated areas, different zones of (changing) temperatures were observed (Fig. 5): A central, initially deformed but ultimately round to almost elliptical hot spot zone directly around the probe tip with a clear border. This zone is surrounded by a rather gradually colored halo-like outer rim with lower temperatures, visually distinguishable by two color zones (in our settings white and yellow-orange). The overall visual thermographic appearance was comparable between RFA and MWA but with a more pronounced shape deformation near large vessels in RFA. This visual impression of a possible heat sink effect was confirmed by temperature profile analysis, where thermography depicted a significant mean surface temperature loss in central vs. peripheral RFA, while there was no statistical difference in MWA. Hereby, we could demonstrate that there is indeed an observable heat sink effect using RFA next to large, perfused vessels (Figs. 5 and 6). This further supports existing evidence, that RFA is more dependent on vascular blood flow, than MWA (15-18). Concerning MWA, data in the literature are rather diverse. Some authors did not find a heat-sink-effect (15,19), while others described it indeed detectable but less pronounced compared to RFA (20-22). Thorough analysis of these studies however reveals, that not only the principal technique (MWA or RFA) used for ablation, but also the needle design affects the magnitude of an observed heat-sink-effect. For example, monopolar MWA and bipolar RFA show comparably low susceptibility, while monopolar RFA seems very strongly affected (8,10). In an experimental study Ringe *et al* showed, that there is a distance- and flow-dependent significant heat-sink-effect when using a 915 MHz MWA system with 45 W for 10 min ablations (15), whereas others found no influence of vascular proximity or flow rate when using a 2.45 GHz 100 W MWA system (23) identical to the equipment we used in the present study. The present experimental data and growing evidence for technical and procedural advantages of MWA encouraged us to increasingly use MWA instead of RFA during surgery (4).

Although CT-/MRI-guided, software-navigated percutaneous ablation (24) with continuous imaging control represents the most sophisticated ablation technique currently available in clinical radiology, distribution of this elaborate method is still limited in most countries. Furthermore, percutaneous ablation of a tumor located at the liver surface or adjacent to vulnerable structures might be technically not feasible. On the contrary, open surgical ablation is fast and affordable and enables the surgeon to rotate the liver within its anatomical surrounding, manually protect heat-sensitive organs (bowel), easily conduct repeated overlapping ablations for a clustered ablation area and also allows for instant complication management e.g., in the case of bleeding or accidental bowel injury.

Effective tumor ablation thereby depends on accurate needle placement in a three-dimensional space, appropriate tissue-destructive energy and sufficient overlapping safety margins (4-10 mm). Local recurrence rates and hepatic progression free survival are usually compared to the gold standard of surgical resection, especially as researchers attribute local recurrences at the ablation site to either insufficient imaging control or the heat-sink-effect. This is of particular relevance when ablation is used in a curative setting as an alternative to resection e.g., in an 'ablate & resect'-strategy for small and deep lesions, aiming to preserve healthy liver parenchyma. Exemplary local recurrence rates after open surgical MWA of colorectal cancer metastasis are in the range of 2-4% in most studies and comparable to those after resection, but may be higher depending on factors such as tumor size (4). Percutaneous and laparoscopic ablations show much more variable local recurrence rates of usually between 5 and 14%. Occasionally, some studies reported even higher local recurrence rates up to 52%, which is probably a result of widely differing inclusion criteria and obvious technical limitations of these approaches (8,25,26). In summary, preventing local recurrence after MWA or RFA is a major issue

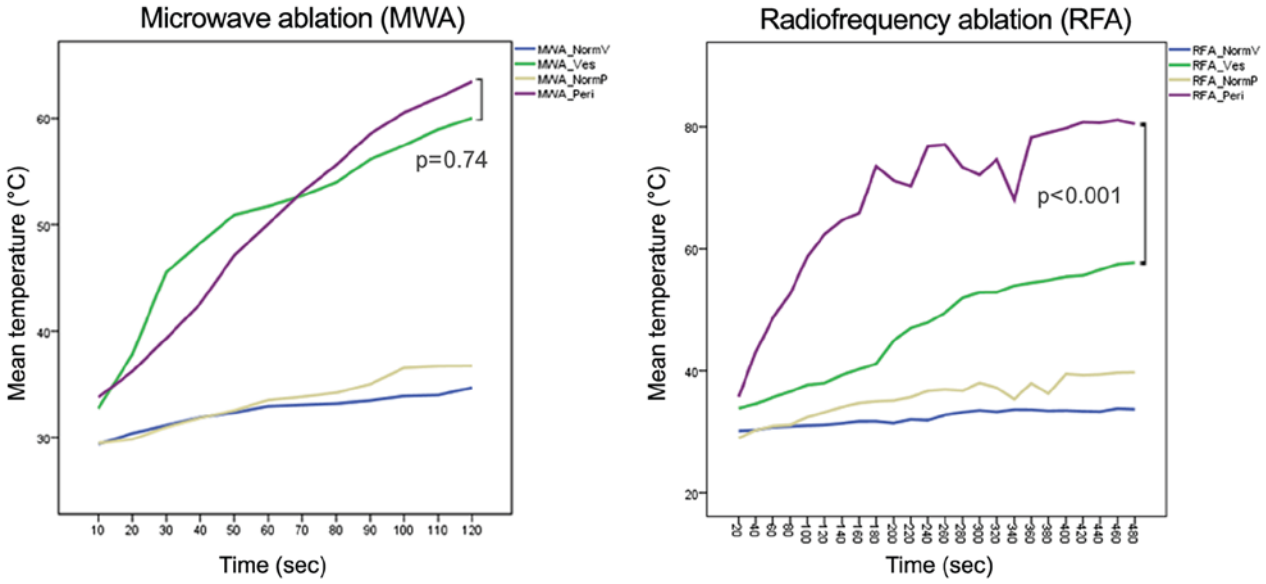

Figure 6. Infrared surface temperature for MWA and RFA. Mean temperature recordings for MWA (left) and RFA (right). In both diagrams, the mean temperature of central (MWA_Ves/RFA_Ves) and peripheral (MWA_Peri/RFA_Peri) ablations are compared to the surrounding baseline temperature of non-ablated parenchyma (MWA/RFA_NormV/MWA/RFA_NormP). RFA, radiofrequency ablation; MWA, microwave ablation.

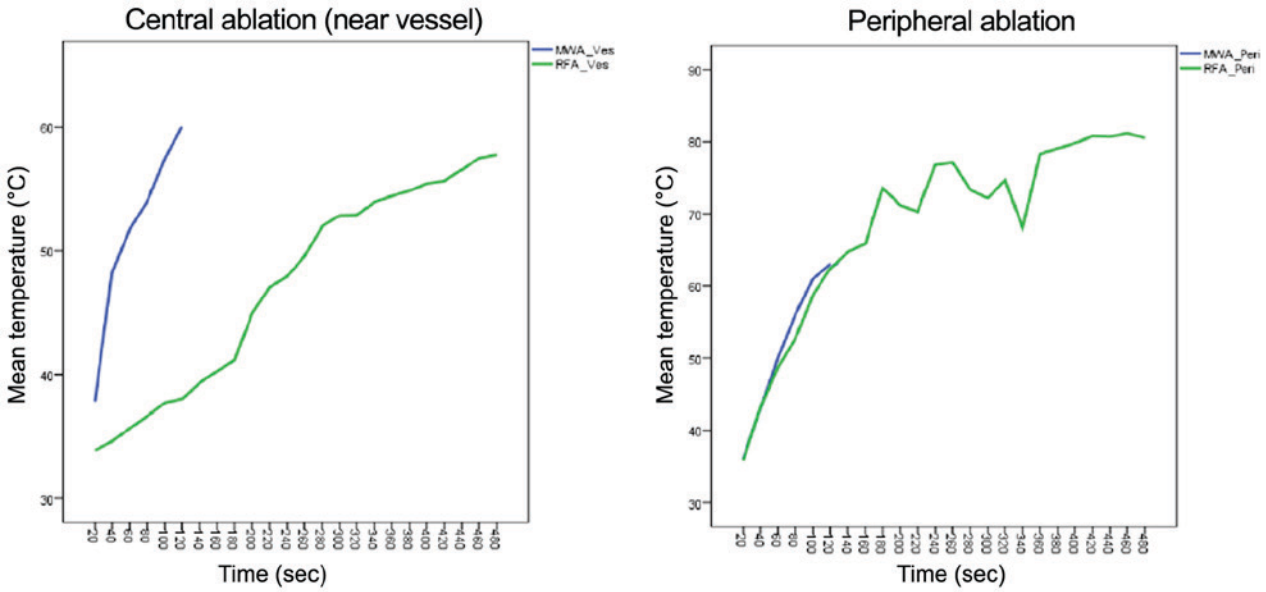

Figure 7. Infrared surface temperature in central and peripheral ablations. Mean temperature recordings comparing MWA with RFA in a central (left) and peripheral (right) ablation setting. MWA is finished after 2 min due to technical reasons. RFA, radiofrequency ablation; MWA, microwave ablation.

in ablative therapies, and several tools have been investigated for this purpose.

Most data is available on contrast-enhanced ultrasound (CEUS), which facilitates a pictorial real-time process of tumor vascularity. CEUS relies on bolus injection of contrast agents consisting of microbubbles (e.g., SonoVue; Bracco SpA, Milan, Italy). Hereby, viable tumor tissue becomes better delineated, which is especially useful for small lesions and steatotic livers. However, gas bubble formation and interference with the RF generator during ablation also compromise CEUS. (12) Furthermore, microbubbles disrupt after some min, reducing the enhancement period and the time frame for needle placement and successful ablation (27). As a result, appropriate application is very much user dependent, usually requiring a well-trained radiologist or surgeon in the operating theatre. In an experimental rat liver model, CEUS optimally determines the maximum dimension of the ablated zone ideally 2 h after RFA, which might further limit its intraoperative use. (11) Other tools such as real-time ultrasound elastography (12) and electrode vibration elastography (13) also seem promising, but are either technically complex, cost intensive or have so far only been evaluated in small series.

The benefits of infrared thermography are its non-invasive nature, the 'user-friendly' real-time visualization and the reasonable cost effectiveness since it is a well-established

technology and not dependent on consumable materials. Another possible field for the clinical use of thermography application could be in delineating the extent of overlapping ablations, since these are particularly challenging to monitor with sonography due to gas bubble formation and scarring. Thermography may also be valuable in raising alertness for heat transmission to nearby, vulnerable structures (bile ducts, bowel loops, diaphragm) (Fig. 5) and unmask technical issues immediately during the ablation process.

This experimental study and the use of thermography for ablations in general have several possible limitations. Firstly, thermographic measurements are derived from surface temperatures. Naturally, these do not necessarily always correlate with the actual temperature in the whole object. However, in an object with distinctive heat conduction such as the human liver it may give a reasonable, reproducible approximation of nearby tissue temperatures. Due to the anatomy of porcine livers with rather flat hepatic parenchyma, extrapolating the investigated effect to deep intraparenchymal ablations e.g., in segment 8 of a human liver might be difficult. Presumably this will have a noticeable impact on surface temperatures and consecutive infrared data and will need further evaluation.

Secondly, we used PBS solution to simulate hepatic blood flow, which might have different conductive properties than whole blood, possibly affecting the results of RFA-which relies on current flux- and might also influence heat transmission to the liver surface and resulting thermographic images. Furthermore, a simplified constant flow rate of 5.3 l/min may not reflect real-life intraoperative variations in hepatic flow, which are dependent on several factors such as heart rate, intravascular volume, blood composition, etc (28,29). However, similar simplified models were used in other published studies examining heat sink effects and different ablation techniques (8).

To overcome these limitations, the next step in evaluating non-invasive thermographic monitoring for hepatic tumor ablation should record the process in an *in vivo* clinical, intraoperative setting. First, we suggest examining temperature profiles in a series of superficial and deep intraparenchymal tumor ablations to standardize surface temperatures. Comparison and/or image-fusion of thermography with intraoperative (contrast-enhanced) ultrasound would be preferable to assess the practical applicability in daily routine.

In conclusion, this study for the first time confirmed infrared thermography as a feasible tool for real-time visualization of open MWA and RFA. Also, we have observed a distinct heat-sink effect in RFA compared to MWA during ablation near large vessels in real time. Further studies and *in-vivo* observations are necessary to estimate its usefulness in daily clinical routine.

Acknowledgements

This study was financially supported by the Austrian Cancer Aid (Österreichische Krebshilfe). The results of this study were presented at the 2014 ESSO Congress (European Society of Surgical Oncology, Liverpool, UK) and the 38th Meeting of the Austrian Society of Surgical Research (Salzburg, Austria).

References

1. Evrard S, Poston G, Kissmeyer-Nielsen P, Diallo A, Desolneux G, Brouste V, Lalet C, Mortensen F, Stättner S, Fenwick S, *et al*: Combined ablation and resection (CARe) as an effective parenchymal sparing treatment for extensive colorectal liver metastases. PLoS One 9: e114404, 2014.
2. Poulou LS, Botsa E, Thanou I, Ziakas PD and Thanos L: Percutaneous microwave ablation vs radiofrequency ablation in the treatment of hepatocellular carcinoma. World J Hepatol 7: 1054-1063, 2015.
3. Molla N, AlMenieir N, Simoneau E, Aljiffry M, Valenti D, Metrakos P, Boucher LM and Hassanain M: The role of interventional radiology in the management of hepatocellular carcinoma. Curr Oncol 21: e480-e492, 2014.
4. Stättner S, Primavesi F, Yip VS, Jones RP, Öfner D, Malik HZ, Fenwick SW and Poston GJ: Evolution of surgical microwave ablation for the treatment of colorectal cancer liver metastasis: Review of the literature and a single centre experience. Surg Today 45: 407-415, 2015.
5. Goldberg SN, Gazelle GS and Mueller PR: Thermal ablation therapy for focal malignancy: A unified approach to underlying principles, techniques, and diagnostic imaging guidance. AJR Am J Roentgenol 174: 323-331, 2000.
6. Hänsler J, Neureiter D, Strobel D, Müller W, Mutter D, Bernatik T, Hahn EG and Becker D: Cellular and vascular reactions in the liver to radio-frequency thermo-ablation with wet needle applicators. Study on juvenile domestic pigs. Eur Surg Res 34: 357-363, 2002.
7. Brace CL: Microwave tissue ablation: Biophysics, technology, and applications. Crit Rev Biomed Eng 38: 65-78, 2010.
8. Pillai K, Akhter J, Chua TC, Shehata M, Alzahrani N, Al-Alem I and Morris DL: Heat sink effect on tumor ablation characteristics as observed in monopolar radiofrequency, bipolar radiofrequency, and microwave, using ex vivo calf liver model. Medicine (Baltimore) 94: e580, 2015.
9. Lubner MG, Brace CL, Hinshaw JL and Lee FT Jr: Microwave tumor ablation: Mechanism of action, clinical results, and devices. J Vasc Interv Radiol 21 (8 Suppl): S192-S203, 2010.
10. Dodd GD III, Dodd NA, Lanctot AC and Glueck DA: Effect of variation of portal venous blood flow on radiofrequency and microwave ablations in a blood-perfused bovine liver model. Radiology 267: 129-136, 2013.
11. Wu H, Wilkins LR, Ziats NP, Haaga JR and Exner AA: Real-time monitoring of radiofrequency ablation and postablation assessment: Accuracy of contrast-enhanced US in experimental rat liver model. Radiology 270: 107-116, 2014.
12. Wiggermann P, Brünn K, Rennert J, Loss M, Wobser H, Schreyer AG, Stroszczynski C and Jung EM: Monitoring during hepatic radiofrequency ablation (RFA): Comparison of real-time ultrasound elastography (RTE) and contrast-enhanced ultrasound (CEUS): First clinical results of 25 patients. Ultraschall Med 34: 590-594, 2013.
13. Dewall RJ, Varghese T and Brace CL: Visualizing ex vivo radiofrequency and microwave ablation zones using electrode vibration elastography. Med Phys 39: 6692-6700, 2012.
14. Ring EF and Ammer K: Infrared thermal imaging in medicine. Physiol Meas 33: R33-R46, 2012.
15. Ringe KI, Lutat C, Rieder C, Schenk A, Wacker F and Raatschen HJ: Experimental evaluation of the heat sink effect in hepatic microwave ablation. PLoS One 10: e0134301, 2015.
16. Chinn SB, Lee FT Jr, Kennedy GD, Chinn C, Johnson CD, Winter TC III, Warner TF and Mahvi DM: Effect of vascular occlusion on radiofrequency ablation of the liver: Results in a porcine model. AJR Am J Roentgenol 176: 789-795, 2001.
17. Kim YS, Rhim H, Cho OK, Koh BH and Kim Y: Intrahepatic recurrence after percutaneous radiofrequency ablation of hepatocellular carcinoma: Analysis of the pattern and risk factors. Eur J Radiol 59: 432-441, 2006.
18. Al-Alem I, Pillai K, Akhter J, Chua TC and Morris DL: Heat sink phenomenon of bipolar and monopolar radiofrequency ablation observed using polypropylene tubes for vessel simulation. Surg Innov 21: 269-276, 2014.
19. Brannan JD and Ladtkow CM: Modeling bimodal vessel effects on radio and microwave frequency ablation zones. Conf Proc IEEE Eng Med Biol Soc 2009: 5989-5992, 2009.
20. Wright AS, Sampson LA, Warner TF, Mahvi DM and Lee FT Jr: Radiofrequency versus microwave ablation in a hepatic porcine model. Radiology 236: 132-139, 2005.

21. Yu NC, Raman SS, Kim YJ, Lassman C, Chang X and Lu DS: Microwave liver ablation: Influence of hepatic vein size on heat-sink effect in a porcine model. J Vasc Interv Radiol 19: 1087-1092, 2008.
22. Bhardwaj N, Strickland AD, Ahmad F, El-Abassy M, Morgan B, Robertson GS and Lloyd DM: Microwave ablation for unresectable hepatic tumours: Clinical results using a novel microwave probe and generator. Eur J Surg Oncol 36: 264-268, 2010.
23. Awad MM, Devgan L, Kamel IR, Torbensen M and Choti MA: Microwave ablation in a hepatic porcine model: Correlation of CT and histopathologic findings. HPB (Oxford) 9: 357-362, 2007.
24. Bale R, Widmann G, Schullian P, Haidu M, Pall G, Klaus A, Weiss H, Biebl M and Margreiter R: Percutaneous stereotactic radiofrequency ablation of colorectal liver metastases. Eur Radiol 22: 930-937, 2012.
25. Hori T, Nagata K, Hasuike S, Onaga M, Motoda M, Moriuchi A, Iwakiri H, Uto H, Kato J, Ido A, *et al*: Risk factors for the local recurrence of hepatocellular carcinoma after a single session of percutaneous radiofrequency ablation. J Gastroenterol 38: 977-981, 2003.
26. Poon RT, Ng KK, Lam CM, Ai V, Yuen J and Fan ST: Effectiveness of radiofrequency ablation for hepatocellular carcinomas larger than 3 cm in diameter. Arch Surg 139: 281-287, 2004.
27. Minami Y and Kudo M: Review of dynamic contrast-enhanced ultrasound guidance in ablation therapy for hepatocellular carcinoma. World J Gastroenterol 17: 4952-4959, 2011.
28. Schutt DJ and Haemmerich D: Effects of variation in perfusion rates and of perfusion models in computational models of radio frequency tumor ablation. Med Phys 35: 3462-3470, 2008.
29. Jakab F, Sugár I, Ráth Z, Nágy P and Faller J: The relationship between portal venous and hepatic arterial blood flow. I. Experimental liver transplantation. HPB Surg 10: 21-26, 1996.

This work is licensed under a Creative Commons Attribution 4.0 International (CC BY 4.0) License.